Drought-Induced Xylem Embolism Limits the Recovery of Leaf Gas Exchange in Scots Pine[1][OPEN]

Romy Rehschuh,[a,2,3] Angelica Cecilia,[b] Marcus Zuber,[b] Tomáš Faragó,[b] Tilo Baumbach,[b] Henrik Hartmann,[c] Steven Jansen,[d] Stefan Mayr,[e] and Nadine Ruehr[a]

[a]Karlsruhe Institute of Technology, KIT Campus Alpin, Institute of Meteorology and Climate Research- Atmospheric Environmental Research, 82467 Garmisch-Partenkirchen, Germany
[b]Karlsruhe Institute of Technology, Institute for Photon Science and Synchrotron Radiation, 76344 Eggenstein-Leopoldshafen, Germany
[c]Max Planck Institute for Biogeochemistry, Department of Biogeochemical Processes, 07745 Jena, Germany
[d]Ulm University, Institute of Systematic Botany and Ecology, 89081 Ulm, Germany
[e]University of Innsbruck, Institute of Botany, 6020 Innsbruck, Austria

ORCID IDs: 0000-0001-9140-0306 (R.R.); 0000-0002-2429-6171 (M.Z.); 0000-0002-9926-5484 (H.H.); 0000-0002-4476-5334 (S.J.); 0000-0002-3319-4396 (S.M.); 0000-0001-5989-7463 (N.R.).

Climate change increases the occurrence of prolonged drought periods with large implications for forest functioning. Scots pine (*Pinus sylvestris*) is one of the most abundant conifers worldwide, and evidence is rising that its resilience to severe drought is limited. However, we know little about its ability to recover from drought-induced embolism. To analyze postdrought hydraulic recovery, we investigated stress and recovery dynamics of leaf gas exchange, nonstructural carbohydrates, and hydraulic properties in 2.5-year-old Scots pine seedlings. We quantified the degree of xylem embolism by combining in vivo x-ray microtomography with intrusive techniques including measurements of hydraulic conductivity and dye staining during drought progression and short-term (2 d) and long-term (4 weeks) recovery. Seedlings were grown under controlled conditions, and irrigation was withheld until stomata closed and xylem water potential declined to −3.2 MPa on average, causing a 46% loss of stem hydraulic conductivity. Following drought release, we found a gradual recovery of leaf gas exchange to 50% to 60% of control values. This partial recovery indicates hydraulic limitations due to drought-induced damage. Whereas xylem water potential recovered close to control values within 2 d, both x-ray microtomography and intrusive measurements revealed no recovery of stem hydraulic conductivity. Moreover, we did not find indications for nonstructural carbohydrate reserves limiting hydraulic recovery. Our findings demonstrate that Scots pine is able to survive severe drought and to partially recover, although we assume that xylem development during the next growing season might compensate for some of the hydraulic impairment. Such drought-induced legacy effects are important when considering vegetation responses to extreme events.

Forests play a key role in the earth system by maintaining hydrological cycles, storing carbon, and providing various ecosystem services (Watson et al., 2018; Jonsson et al., 2019). However, with increasingly frequent occurrences of climate extremes and particularly drought events, these pivotal services of forests are at risk (Choat et al., 2012; Reichstein et al., 2013). Additionally, severe drought events can result in forest decline, as has been observed worldwide (Allen et al., 2015; Adams et al., 2017; Buras et al., 2018; Hartmann et al., 2018). Often, trees do not die during the stress event but may succumb weeks to years later, and gymnosperms were found to show larger drought legacy effects than angiosperms (Anderegg et al., 2015b; DeSoto et al., 2020). Stress-induced functional damage may persist by incomplete recovery of plant hydraulic and metabolic processes (Trugman et al., 2018; Ruehr et al., 2019), making trees vulnerable (McDowell, 2011) to pests and pathogen attacks (Allen et al., 2015; Rehschuh et al., 2017). Due to the important role of recovery in stress resilience and tree survival, the physiological mechanisms associated with drought recovery and carryover effects require more attention.

The time necessary for complete recovery of physiological functioning is crucial for tree survival, because further stress events could affect trees even more

[1]This work was supported by the German Research Foundation-Emmy Noether Program (grant no. RU 1657/2–1) and by the Austrian Science Fund (grant no. I3724–B32).

[2]Senior author.

[3]Author for contact: romy.rehschuh@kit.edu.

The author responsible for distribution of materials integral to the findings presented in this article in accordance with the policy described in the Instructions for Authors (www.plantphysiol.org) is: Romy Rehschuh (romy.rehschuh@kit.edu).

R.R. and N.R. designed the study with support from S.J., S.M., and H.H.; R.R. and N.R. conducted the experiments; R.R., A.C., M.Z., T.F., and N.R. performed micro-CT measurements and analyses, and T.B. supervised the measurements; H.H. conducted NSC analyses and R.R. performed all other measurements and analyzed the data with support from N.R, S.M., H.H., and S.J.; R.R. and N.R. wrote the article with contributions from all coauthors.

[OPEN]Articles can be viewed without a subscription.

www.plantphysiol.org/cgi/doi/10.1104/pp.20.00407

strongly (Schwalm et al., 2017). In addition, the severity of stress is an important factor influencing recovery dynamics (Ruehr et al., 2019). Hence, we can assume that recovery is slow when drought stress impairs critical plant physiological processes, such as carbon uptake or water transport. Recent studies have revealed that the damage to the plant hydraulic system plays a critical role in impeding plant survival during drought (Anderegg et al., 2015a; Salmon et al., 2015; Adams et al., 2017; Choat et al., 2018) as well as affecting postdrought recovery (Choat et al., 2019; Ruehr et al., 2019), but it needs to be proven if hydraulic impairment is one of the main factors preventing or postponing full recovery of vital physiological processes in the long term (Körner, 2019).

Drought periods limit tree water uptake and cause plants to close stomata to prevent excessive water loss from transpiration and thus critical water potentials (Meinzer, 2002; Martínez-Vilalta et al., 2004). If drought persists, trees will continue to dehydrate and the water potential will decline. Below a critical threshold, large gas bubbles can be formed in the water-conducting pathway of the xylem, and the resulting embolism may spread to neighboring water-filled conduits via pit membranes (Sperry and Tyree, 1988; Tyree and Sperry, 1989; Kaack et al., 2019). Consequently, the hydraulic conductivity of embolized xylem tissue will be impaired, leading to reduced leaf water supply and ultimately to stomatal limitation and reduction of carbon uptake (Nardini and Salleo, 2000; Nardini et al., 2017), thus affecting nonstructural carbohydrate (NSC) storage pools (McDowell, 2011).

There is clear evidence for seasonal and daily refilling of embolized conduits in some angiosperm species based on positive xylem pressure at the local or whole-plant level (Leng et al., 2013; Charrier et al., 2016; Gleason et al., 2017). A frequently cited assumption is that refilling is largely driven by the active transport and osmotic exudation of inorganic ions, sugars, or larger organic molecules into embolized conduit lumina (Taiz et al., 2014; Nobel, 2020). Alternatively, osmotic agents (e.g. sugars and degraded starch) could be mainly concentrated in parenchyma cells that are directly connected to embolized conduits, resulting in increased turgor pressure in these parenchyma cells and water flow by osmotic pressure (Canny, 1998; Pickard, 2003). Nevertheless, the exact mechanisms behind positive xylem pressure remain unknown. Although conifers, which have no vessels and low levels of parenchyma in their xylem tissue (Johnson et al., 2012; Morris et al., 2016), have also been reported to refill embolism (Laur and Hacke, 2014; Klein et al., 2016; Tomasella et al., 2017), a growing body of literature indicates a lack of refilling capability in most conifer species (Utsumi et al., 2003; Brodribb et al., 2010; Choat et al., 2015). Moreover, instead of developing the ability to generate positive xylem pressure, conifers may prevent embolism by early stomatal closure during drought, regain hydraulic conductivity by quickly growing new xylem during recovery (Brodribb et al., 2010; Hammond et al., 2019), or use another, yet unknown, refilling mechanism. *Picea abies*, for instance, shows severe levels of embolism by freeze-thaw cycles during winter but refilling during spring, which could be associated with water uptake via needles and bark tissue (Mayr et al., 2014, 2020).

Observations of embolism could also be hampered by artifacts associated with hydraulic conductivity measurements, such as bubble formation by cutting of xylem under negative pressure and artificial refilling of embolized conduits (Wheeler et al., 2013; De Baerdemaeker et al., 2019). For this reason, nonintrusive methods provide a welcoming alternative to visualize the hydraulic status of xylem conduits in vivo. Examples include the application of magnetic resonance imaging (Holbrook et al., 2001; Bouda et al., 2019) and x-ray microtomography (micro-CT; Brodersen et al., 2010; Choat et al., 2015, 2016, 2019; Nardini et al., 2017). The application of these high-tech methods has become increasingly popular in recent years, providing novel insights into the ability of plants to recover embolized conduits following release from drought.

In recent years, Scots pine (*Pinus sylvestris*), one of the most abundant conifer species worldwide, has exhibited increasing mortality rates in many regions of Europe (Rigling et al., 2013; Salmon et al., 2015; Buras et al., 2018; Etzold et al., 2019). This is surprising because Scots pine is considered to be relatively drought tolerant based on its isohydric stomatal behavior causing stomata to close early during drought (Martínez-Vilalta et al., 2004). A likely explanation is that Scots pine, typically occurring on the driest sites in commercially used forests of Central Europe, may be pushed beyond its physiological limits by more frequent and more severe drought events during the last decades. In light of these recent developments, an improved physiological understanding of the ability of Scots pine to tolerate drought and to recover hydraulic and metabolic functioning post drought is urgently needed.

The interaction of the recovery of leaf gas exchange and xylem hydraulic functioning has rarely been analyzed over the long term (1 month following drought release) using hydraulic intrusive and nonintrusive methods. In this study, we analyzed tree physiological questions while testing methodological agreements. To elucidate the mechanisms governing postdrought recovery, we exposed 2.5-year-old Scots pine seedlings to a severe drought stress, which resulted in ~50% loss of hydraulic conductivity (PLC), rewatered them, and followed their recovery trajectories for 4 weeks. We then assessed whether the hydraulic system can be repaired via xylem refilling in the short term (2 d after rewatering) and in the long term (4 weeks after rewatering). For this, we measured in vivo embolism spread using micro-CT as well as stem hydraulic conductivity (K_S) of stem segments using a pressure-flow method and performed dye-staining experiments. To relate hydraulic functioning to seedling carbon metabolism,

we determined leaf gas-exchange dynamics and NSC concentrations of needle, stem, and root tissues. We hypothesized a delayed recovery of leaf gas exchange due to an impaired hydraulic system by drought. In case of embolism reversal, we expected the degradation of starch into soluble sugars to lower the osmotic potential in embolized conduits, thus allowing for refilling. Furthermore, we expected agreement between the destructive and nondestructive methods used to test for hydraulic recovery.

RESULTS

Responses of Leaf Gas Exchange and Xylem Water Potential during Drought and Postdrought Recovery

Leaf gas exchange in Scots pine seedlings was sensitive to drought and declined progressively with decreasing xylem water potential (Ψ_{Xylem}; Tukey's honestly significant difference test [HSD], $P < 0.001$; Fig. 1, A–D), whereas leaf gas exchange in the seedlings of the control treatment showed little variation. Stomatal conductance (g_s) was almost zero about 28 d after the drought treatment was initiated when Ψ_{Xylem} declined below −2 MPa. Simultaneously, relative needle water content (RWC_{Needle}) decreased with drought progression to 66% (compared with RWC_{Needle} of 80% in control seedlings; Tukey's HSD, $P < 0.001$; Fig. 1E) when Ψ_{Xylem} was as low as −3.2 ± 0.2 MPa on the last day of the drought treatment (Fig. 1D). This relates to about 50% PLC based on vulnerability curves (Supplemental Fig. S1). Despite this severe drought treatment, we did not observe browning or loss of needles.

After drought seedlings were rewatered on day 0 (see Supplemental Fig. S2 for environmental conditions), we observed an initial increase in leaf gas exchange, which subsided about 9 d later (Fig. 1, A–C). After 27 d, A_{SAT} had recovered to 57% of control values, whereas g_s and E reached about 50% (Tukey's HSD, $P < 0.001$; Table 1). This resulted in intrinsic water-use efficiency (WUE_i) to increase by 19% in previously drought-treated seedlings.

In contrast to gas-exchange rates, Ψ_{Xylem} recovered much faster and reached −1.25 MPa 2 d after rewatering. Throughout the following 25 d of recovery, the difference in Ψ_{Xylem} between the control and drought treatments remained relatively constant, and hence seedlings recovering from drought did not reach the Ψ_{Xylem} of control seedlings (Tukey's HSD, $P < 0.001$). The recovery trajectory of RWC_{Needle} appeared to differ from that of Ψ_{Xylem} with a much slower increase, but it reached control values at the end of the experiment.

Dynamics of NSC

The drought-induced decrease in photosynthesis and Ψ_{Xylem} was mirrored by NSC dynamics, which showed

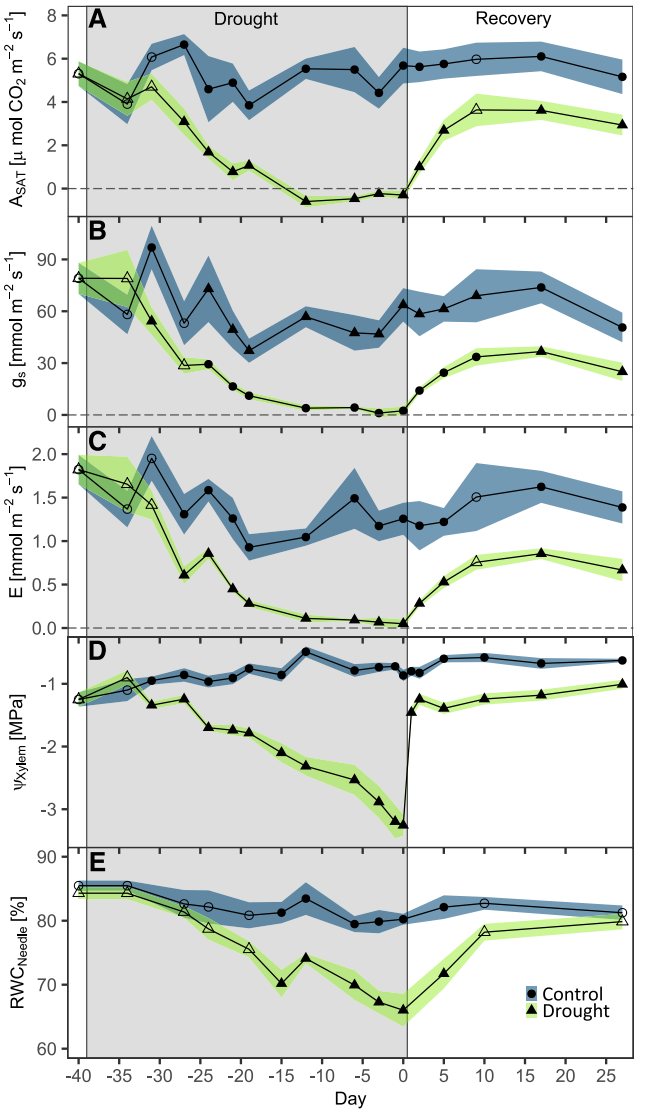

Figure 1. Dynamics of leaf gas exchange and water relations during drought and recovery. Shown are light-saturated photosynthesis (A_{SAT}; A), g_s (B), transpiration (E; C), Ψ_{Xylem} (D), and RWC_{Needle} (E) during drought (gray area) and recovery. Data are treatment averages, and shaded areas are ±SE; $n = 6$ control and $n = 10$ to 12 drought-recovery seedlings. Filled symbols indicate significant differences between treatments (Wilcoxon rank-sum test). Seedlings were rewatered in the evening of day 0. From day 5 onward, only those seedlings experiencing a slightly longer drought phase were measured.

a significant decline by 80% to 95% in starch concentrations of all tissues studied (Fig. 2, C and D; Table 2). In contrast to starch, soluble sugar concentrations seemed to be unaffected by drought in needles and bark (Fig. 2, A and B).

Following rewatering, soluble sugars showed an initial decline in all tissues compared with the control, followed by a pronounced increase 5 d after rewatering. Simultaneously, we found the most pronounced increases of starch concentrations in needle and root tissues, which tripled compared with those of control

Table 1. *Treatment effect (TE) between control and drought seedlings at the end of the drought period and after the 27-d recovery period*

Shown are gas-exchange parameters A_{SAT}, g_s, and E as well as Ψ_{Xylem}, RWC_{Needle}, and WUE_i. Values are treatment averages ± SE (n = 6 control and n = 10–12 drought-recovery seedlings). –, Treatment effects do not apply to control data.

Parameter	Treatment	End of Stress	TE	End of Recovery Period	TE
			%		%
A_{SAT} (μmol CO_2 m^{-2} s^{-1}])	Control	5.7 ± 0.8	–	5.2 ± 0.8	–
	Drought	−0.3 ± 0.1	−105.2	3.0 ± 0.5	−43.1
g_s (mmol m^{-2} s^{-1})	Control	63.7 ± 9.7	–	50.6 ± 8.6	–
	Drought	2.4 ± 2.4	−96.2	25.0 ± 5.3	−50.7
E (mmol m^{-2} s^{-1})	Control	1.3 ± 0.2	–	1.4 ± 0.2	–
	Drought	0.05 ± 0.05	−96.0	0.67 ± 0.1	−51.9
WUE_i (μmol mol^{-1})	Control	94.9 ± 15.6	–	103.7 ± 4.2	–
	Drought	290.5 ± 213.6	206.1	123.1 ± 10.1	18.7
Ψ_{Xylem} (MPa)	Control	−0.87 ± 0.1	–	−0.63 ± 0.03	–
	Drought	−3.25 ± 0.2	−275.7	−1.00 ± 0.1	−60.6
RWC_{Needle} (%)	Control	80.2 ± 0.9	–	81.2 ± 1.1	–
	Drought	66.0 ± 2.6	−17.7	79.9 ± 1.2	−1.7

seedlings (Fig. 2C). Interestingly, this increase in sugar and starch concentrations initially followed the recovery trajectory of photosynthesis (Fig. 1A) but vanished 4 weeks after rewatering (Fig. 2). One exception was a persistent high level of starch in needles and an accumulation in the bark compared with the control seedlings. Dynamics in starch concentrations seemed to be closely linked to Ψ_{Xylem} (Supplemental Fig. S3F), likely due to a drought-related suppression of carbon uptake.

Hydraulic Conductivity and Xylem Embolism

We tested the ability of Scots pine to refill embolized conduits using independent approaches: (1) visual assessment of water- versus air-filled conduits in vivo using micro-CT; (2) observation of conductive xylem area via dye staining; and (3) measurements of K_S using a pressure-flow technique.

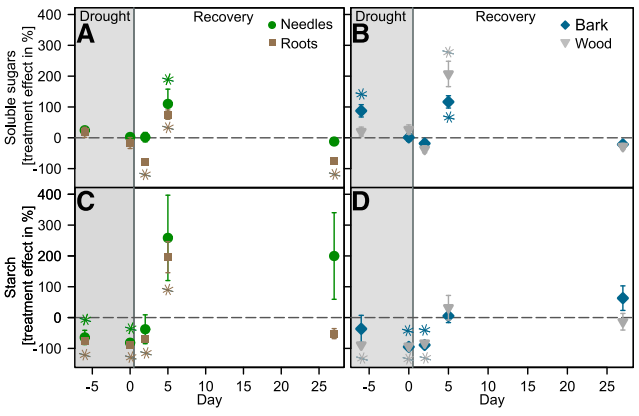

Figure 2. NSC dynamics during drought and recovery. Tissue-specific soluble sugar (A and B) and starch (C and D) concentrations of the drought treatment are shown as treatment effects in percentage of control values ± SE (n = 5–8 per tissue and treatment). The dashed horizontal lines indicate the mean of the control treatment. Asterisks indicate significant differences from the control treatment derived from the concentrations measured (Wilcoxon rank-sum test). The gray boxes represent the last week of the drought period; seedlings were rewatered in the evening of day 0.

Micro-CT images revealed that drought (average Ψ_{Xylem} = −3.2 ± 0.2 MPa) resulted in ~28% ± 3% dysfunctional, air-filled xylem area (Fig. 3B; for additional micro-CT images, see Supplemental Fig. S4), which manifested mainly in the latewood (on average ~70% of embolized tracheid area). The embolized areas were most pronounced in tracheids of the first growth ring (near the pith) and in a distinct concentric ring of latewood tracheids in the second-year growth ring. Under progressive levels of drought, they also occurred in the earlywood of the second year and in the most recently developed tracheids of earlywood and latewood. The xylem of control seedlings appeared generally functional, with a small fraction of ~4% nonconducting tracheids, of which ~85% were present in the latewood. Embolized tracheids occurred mainly close to the pith and also in the second-year latewood ring (Fig. 3A; Supplemental Fig. S4, A–C).

Following rewatering, when Ψ_{Xylem} had recovered to −1.25 ± 0.08 MPa 2 d later (Fig. 1D), we remeasured two-thirds of the previously analyzed drought-recovery seedlings. We could not detect indications of embolism reversal, and the patterns of dysfunctional xylem area remained similar to the patterns observed before rewatering started (Fig. 3, B and C; Supplemental Fig. S4). Four weeks after rewatering, we remeasured embolism on another set of drought-recovery seedlings (which had been stressed to a similar Ψ_{Xylem} of −3.15 ± 0.1 MPa). Once more, we did not detect any evidence of refilling of embolized xylem area (Fig. 3D; Supplemental Fig. S4, F, I, and M), which was also reflected in calculated PLA (Fig. 4A). In addition, we found that the degree of embolism apparently had no effect on hydraulic recovery, because seedlings that were only stressed to their P_{12} values (the Ψ_{Xylem} at which 12% hydraulic conductivity is lost; here Ψ_{Xylem} of –1.5 to –2.4 MPa) did not show signs of embolism reversal

Table 2. *Absolute values and treatment effect (TE) between control and drought recovery seedlings for the soluble sugar and starch concentrations at the end of the drought period and after a 27-d recovery period*

Values are treatment averages ± SE; n = 5 to 8 per tissue and treatment. –, Treatment effects do not apply to control data.

Parameter	Tissue	Treatment	End of Stress	TE	End of Recovery Period	TE
				%		%
Soluble sugars (mg g^{-1})	Needle	Control	33.1 ± 3.4	–	48.7 ± 7.2	–
		Drought	34.0 ± 2.1	2.6	42.9 ± 3.1	−12.0
	Bark	Control	28.6 ± 3.3	–	52.3 ± 7.2	–
		Drought	28.9 ± 4.3	1.0	41.0 ± 2.3	−21.5
	Wood	Control	4.8 ± 0.6	–	15.1 ± 2.2	–
		Drought	6.1 ± 0.8	26.9	10.8 ± 1.3	−28.2
	Roots	Control	22.0 ± 2.3	–	36.3 ± 2.2	–
		Drought	18.2 ± 5.0	−17.0	8.4 ± 0.9	−76.8
Starch (mg g^{-1})	Needle	Control	5.0 ± 1.4	–	5.3 ± 1.7	–
		Drought	0.9 ± 0.2	−81.6	15.7 ± 3.1	199.7
	Bark	Control	15.8 ± 1.3	–	20.1 ± 8.3	–
		Drought	0.8 ± 0.4	−95.0	32.7 ± 5.5	63.0
	Wood	Control	2.9 ± 1.0	–	2.8 ± 1.2	–
		Drought	0.21 ± 0.04	−92.7	2.4 ± 0.7	−13.5
	Roots	Control	7.9 ± 1.7	–	24.0 ± 8.0	–
		Drought	0.9 ± 0.2	−88.4	11.5 ± 2.0	−52.1

(Supplemental Fig. S4, D–F). The results gained via micro-CT were further confirmed by dye staining, which indicated similar patterns of conducting versus nonconducting xylem areas, showing ~4% nonconducting area in control seedlings compared with ~26% nonconducting area in drought-stressed and recovering seedlings (Supplemental Fig. S5).

We further verified the agreement between micro-CT and the pressure-flow method on a subsample of seedlings previously measured at the synchrotron and on seedlings that were not scanned. K_S declined significantly with drought progression by an average of 46% compared with control seedlings, and neither recovered within 2 d nor within a longer period of 27 d (Fig. 4B).

In addition, we plotted the loss of hydraulic conductivity estimated from pressure-flow analyses and PLA calculated from micro-CT images versus Ψ_{Xylem} at sample taking (Supplemental Fig. S1). Considering PLC from hydraulic measurements, we observed an overall good agreement with the vulnerability curve generated by the Cavitron. Regarding PLA, we found values to lie within the Cavitron vulnerability curve when observing Ψ_{Xylem} up to about –3 MPa. At $\Psi_{Xylem} < -3$ MPa, however, the Cavitron curve showed an earlier increase in PLC at less negative Ψ_{Xylem} than PLA.

In addition, linking NSC concentrations to the hydraulic parameters K_S, PLA, or RWC_{Needle} did not indicate a dependency (Supplemental Fig. S3).

Relationships of Leaf Gas Exchange with Ψ_{Xylem} during Drought and Recovery

We found A_{SAT} (R^2 = 0.68) and g_s (R^2 = 0.63) to be closely related to Ψ_{Xylem} during drought, and stomatal closure was at −2.4 ± 0.5 MPa close to P_{12} (Fig. 5), which corresponded approximately to the Ψ_{Xylem} when embolism started to form (Supplemental Fig. S1). A_{SAT} became negative (i.e. respiration exceeded assimilation rates) slightly earlier at a Ψ_{Xylem} of approximately −1.9 MPa.

The close relationships of A_{SAT} and g_s with Ψ_{Xylem} changed dramatically after rewatering (R^2 = 0.08 and 0.09). At Ψ_{Xylem} of −0.8 MPa, we observed A_{SAT}, g_s, and E to be 43%, 51%, and 52% lower, respectively, in

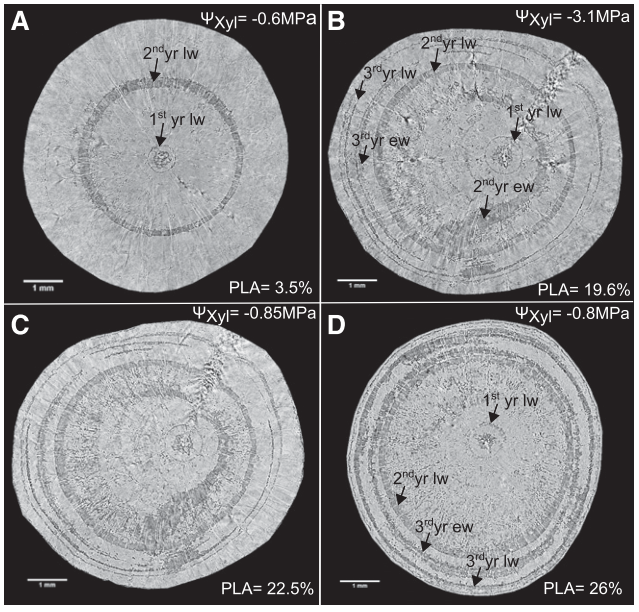

Figure 3. Micro-CT images of Scots pine stems. Shown are examples of transverse slices of stem xylem of a control seedling (A), a drought-stressed seedling (B), the same one 2 d after rewatering (C), and another seedling that was stressed to −3 MPa but analyzed after 4 weeks of rewatering (D). Embolized tracheids appear black and water-filled tracheids are in light gray. Ψ_{Xylem} (Ψ_{Xyl}) before micro-CT measurements and percentage loss of water-conducting area (PLA) are given. Bars = 1 mm.

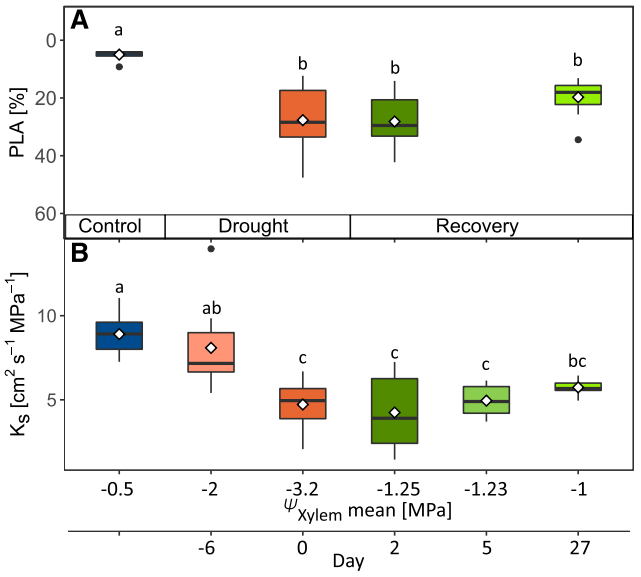

Figure 4. PLA and K_S during drought and recovery. Given are PLA from micro-CT images (A) and K_S from pressure-flow measurements (B) for control (blue), drought (reddish colors), and drought-recovery (greenish colors) seedlings (n = 6–12). Diamonds depict mean values per treatment and time step. Different lowercase letters indicate significant differences between treatments (Kruskal-Wallis test and Bonferroni posthoc test).

drought-recovery seedlings compared with control seedlings (Fig. 5; Table 1). This reduced recovery of carbon assimilation and transpiration compares well with the 46% reduction of K_S in the drought-recovery seedlings (Fig. 4B), indicating that the persistence of xylem embolism was the main reason for the incomplete recovery of leaf gas exchange.

DISCUSSION

The results of our study provide evidence for hydraulic impairments limiting the drought recovery of Scots pine seedlings. Both hydraulic measurements on stem segments and micro-CT imaging on intact seedlings showed that embolized xylem tissue did not recover within 2 d or after 4 weeks following rewatering. Furthermore, we found no indication that carbon reserves were limiting hydraulic recovery. Leaf photosynthesis, E, and g_s also recovered partially. Their recovery was affected by the persistently reduced stem hydraulic conductance, which restricted water transport and hence normal plant functioning.

Drought Results in Hydraulic Limitations Altering Gas Exchange and NSC Dynamics

We dehydrated Scots pine seedlings to about 50% loss of hydraulic conductivity (Fig. 4B), which, as expected, did not result in tree death (Brodribb and Cochard, 2009). In a recent meta-analysis, a PLC higher than 60% was shown to be nonlethal in many tree species, including gymnosperms (Adams et al., 2017), and *Pinus taeda* saplings survived 72% PLC (Hammond et al., 2019). Our P_{50} values generally agreed with previous studies on Scots pine (Martínez-Vilalta et al., 2004; Poyatos et al., 2008; Torres-Ruiz et al., 2016). Torres-Ruiz et al. (2016) reported relatively similar P_{50} values for Cavitron measurements and 50% of embolized tracheid area obtained via micro-CT (−3.3 versus −3 MPa). We found good agreement of PLC derived from Cavitron and pressure-flow analyses (Supplemental Fig. S1). The Cavitron curve, however, showed an earlier reduction in loss of conductivity at less negative Ψ_{Xylem} than PLA calculated from micro-CT

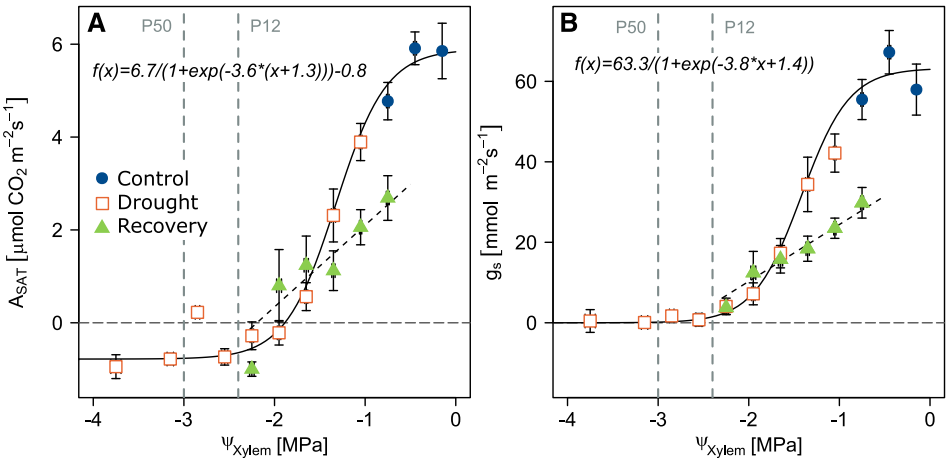

Figure 5. Relationships of leaf gas exchange with Ψ_{Xylem}. Dependencies of A_{SAT} (A) and g_S (B) with Ψ_{Xylem} are given for the control treatment (including prestress data of the drought treatment; blue circles), drought progression (orange squares), and recovery (green triangles). Data are bin averages for intervals of 0.3 MPa, and means ± SE are shown. P_{12} and P_{50} as determined by Cavitron measurements are indicated. A sigmoidal function was fitted to control and drought data (A_{SAT} root-mean-square error = 1.64; g_s root-mean-square error = 20.9) and a linear regression to data of drought seedlings after rewatering (A_{SAT} R^2 = 0.08; g_s R^2 = 0.09).

images. We exclude differences in sampling time as the reason for this discrepancy (Charrier et al., 2018), as pressure-flow measurements compared quite well with the data derived from the Cavitron. The difference could rather be explained by the fact that PLA quantifies embolism visually and directly but does not account for hydraulic conductivity. Therefore, it probably overestimates embolism resistance compared with PLC in our study, as water-filled tracheids, which are poorly connected to other water-filled tracheids, might appear as fully functional.

As shown in various earlier studies (Skelton et al., 2017; Birami et al., 2018), Scots pine reduced leaf gas exchange (A_{SAT}, g_S, and E) during the progression of drought alongside declining Ψ_{Xylem} (Fig. 1, A–D). Stomata of seedlings were fully closed at a Ψ_{Xylem} of approximately −2.4 MPa (Fig. 5B), which reduces water loss via transpiration and delays dehydration. The xylem tensions we observed at stomatal closure lie well within the reported range for pines (Martínez-Vilalta et al., 2004) and closely correspond to P_{12} (generally related to the onset of embolism formation), which is consistent with previous studies (Skelton et al., 2015; Li et al., 2016).

In our study, partial stomatal closure reduced carbon uptake, and with progressing stomatal closure, light respiration exceeded A_{SAT} at $\Psi_{Xylem} < -1.9$ MPa (Fig. 5A). This was further reflected in significantly decreasing starch concentrations in all tissues. By contrast, sugar concentrations did not decrease, as seedlings needed to maintain metabolic and osmoregulatory processes (Fig. 2), likely at the cost of starch and other carbon reserves. With drought progression, sink activity can be reduced earlier than source activity, which leads to an accumulation of sugars in leaves (Muller et al., 2011) and, as transport is slowed during drought, also in the stem phloem. An additional mechanism sustaining sugar concentrations could be woody stem photosynthesis, which allows internal CO_2 recycling independent of stomata opening (Vandegehuchte et al., 2015). Increased sugar concentrations in the wood may favor hydraulic functioning (Tomasella et al., 2019). Although there is no uniform pattern of NSC dynamics during drought (Hartmann and Trumbore, 2016), many previous studies have found starch concentrations to decline (Adams et al., 2017; Birami et al., 2018). This indicates that during drought stress, when net leaf carbon gain is suppressed, trees need to rely on reserve compounds.

No Reversal of Xylem Embolism 4 Weeks Postdrought

Visual assessment via noninvasive micro-CT on Scots pine seedlings allowed for a proper estimation of air-filled versus water-filled areas within the stem xylem. Latewood showed more embolism than earlywood (Fig. 3; Supplemental Fig. S4), which agrees well with other studies on conifers (Mayr and Cochard, 2003; Choat et al., 2015, 2016; Umebayashi et al., 2016), and could be caused by the seemingly inflexible, rigid nature of the pit membrane, which results in a reduced ability to seal the pit aperture to prevent air seeding (Petty and Preston, 1970; Domec and Gartner, 2002; Dalla-Salda et al., 2014). Latewood tracheids frequently show a lower pit density than earlywood, with pit borders reported to be larger than 15 μm in earlywood but only 4 to 6 μm in latewood of *Picea sitchensis* and *Picea orientalis* (Domec et al., 2006; Usta and Hale, 2006). Therefore, quantitative pit characteristics do not seem to explain the low embolism resistance of latewood compared with earlywood. The concentric distribution of embolized tracheids, however, could be explained by the occurrence of bordered pits in radial walls of tracheids (Dalla-Salda et al., 2014; Choat et al., 2016). Most of our control seedlings (and also dehydrated ones) revealed air-filled tracheids in the inner section of the xylem around the pith, which has also been reported previously for well-watered trees (Choat et al., 2016; Torres-Ruiz et al., 2016) and could have resulted from fast wood growth during early developmental stages of the plant, and tracheids with only partial secondary wall thickening.

Drought-recovery seedlings showed no reduction of PLA after 2 d and 4 weeks of rewatering (Figs. 3, B–D, and 4A). As hypothesized, results from the pressure-flow technique and dye staining agreed with micro-CT measurements, revealing that embolized xylem did not refill and hydraulic conductivity did not recover within 4 weeks post drought (Fig. 4). This confirms previous findings on other conifer species. For instance, Choat et al. (2015) reported a lack of refilling in *Sequoia sempervirens* 2 weeks post drought using micro-CT. Furthermore, no evidence of embolism refilling in *Pinus thunbergii* and three other conifer species using cryoscanning electron microscopy was found (Utsumi et al., 2003; Umebayashi et al., 2016). Moreover, Brodribb et al. (2010) detected no evidence of refilling in *Callitris rhomboidea*, as did Hammond et al. (2019) using intrusive methods for *P. taeda*. By contrast, reversal of winter embolism caused by a combination of strong drought and freeze-thaw cycles has been observed repeatedly (McCulloh et al., 2011; Mayr et al., 2014, 2020). In our study, soil drought was released via rewatering of the soil. Other studies, in which needle and bark tissues were rewetted, however, reported at least partial embolism reversal (Laur and Hacke, 2014; Earles et al., 2016). Therefore, the type of rewetting and also the timing of the drought experiment late in the season could play a role in the ability of trees to refill embolized xylem conduits. We did not measure predawn water potential here, but nighttime conditions were relatively cool and moist, presumably preventing water loss by transpiration. Therefore, it is reasonable to assume that atmospheric conditions have not limited the ability to refill embolism in our study. Since the physiological parameters measured in the rewatered seedlings reached a plateau after 27 d, it seems unlikely that refilling would occur after a longer recovery period. Moreover, the time scale of seasonal refilling contrasts

strongly with reports on daily refilling processes in conifers (Klein et al., 2016, 2018), which seems highly unlikely.

Reasons for the lack of xylem refilling may include the low proportion of parenchyma in the secondary xylem and relatively low NSC reserves in stems compared with angiosperms (Johnson et al., 2012; Morris et al., 2016), in which refilling has been proved (Salleo et al., 2009; Charrier et al., 2016; Gleason et al., 2017). In our study, we did not find any evidence of starch mobilization to coincide with rewatering. Directly after stress release, low wood starch concentrations could potentially have limited the lowering of the osmotic potential in the embolized conduit. However, 5 d after rewatering, drought-recovery seedlings had reached similar wood starch concentrations as the control seedlings, and soluble sugar concentrations surpassed the values of control seedlings. In addition, we found no clear relationship between starch and soluble sugar concentrations of relevant tissues with K_S, PLA, or RWC_{Needle} (Supplemental Fig. S3). This indicates that the availability of NSC reserves was not a limiting factor in embolism repair; however, since no refilling occurred in our study, we cannot answer our second hypothesis.

Impaired Hydraulic Functionality Affects Carbon Metabolism Postdrought

Following stress release, we observed leaf gas exchange increasing slowly for about 9 d, then remaining unchanged during the following 2.5 weeks (Fig. 1, A–C). Starch and soluble sugar concentrations increased strongly in all tissues along with carbon uptake 5 d after rewatering (Fig. 2). This may indicate that sink activities (e.g. growth) were still inhibited shortly after stress release. Other studies have shown that reserve formation is associated with a growth inhibition due to low water potentials (Muller et al., 2011) or active up-regulation via the synthesis of starch or lipids (Dietze et al., 2014). Storage formation in needles and bark, which we have observed to occur during recovery, might indicate a conservative strategy to support the survival of subsequent drought periods (Galiano et al., 2017; Weber et al., 2019). Furthermore, storing of NSC in the bark might be important to fuel longitudinal growth and basal area increment of stems in the following year, as has been observed previously for branches (Kagawa et al., 2006), presumably to restore hydraulic conductivity in the long term. By contrast, the observed consumption of root NSC in drought-recovery seedlings might suggest an immediate up-regulation of repair and regrowth of root tissues, indicating the preference of resource investments to restore water and nutrient uptake (Hagedorn et al., 2016; Galiano et al., 2017; Cuneo et al., 2020). To transport assimilates to source organs, functional phloem loading and transport are needed. We observed that starch and soluble sugars increased in root tissues after rewatering, which indicates phloem functionality. This was also supported by the delayed but full recovery of RWC_{Needle}, which might restore the functionality of carbon transport via symplastic loading and unloading (Lalonde et al., 2003). The recovery of RWC_{Needle} indicates the repair of extraxylary tissues (Laur and Hacke, 2014), which also plays an important role in buffering temporary water deficits (Charra-Vaskou et al., 2012).

Considering leaf gas exchange, we found a higher WUE_i in drought-recovery seedlings compared with control seedlings, which has previously been explained by an improved mesophyll conductance following drought release (Cano et al., 2014). In agreement, a meta-analysis found a complete recovery of photosynthesis to be more often reported than that of g_s (Ruehr et al., 2019), which results in a higher WUE_i during recovery than before stress. In our study, we did not observe a complete recovery of A_{SAT} or of g_s throughout the 4-week recovery period, even though Ψ_{Xylem} increased quickly and steeply (Fig. 1). However, Ψ_{Xylem} also did not recover fully, which agrees with findings on severely drought-stressed *C. rhomboidea* (Brodribb et al., 2010). Similar to our study, fast increase of water potential but not leaf gas exchange post drought has been reported in many earlier studies (Ruehr et al., 2019). An initial delay in the recovery of g_s might be the result of abscisic acid, a phytohormone inducing stomatal closure, being maintained at high concentrations in the leaves for several hours after rewetting (Brodribb and McAdam, 2013). Furthermore, impaired biochemical capacity (Cano et al., 2014), metabolic constraints (Hagedorn et al., 2016; Adams et al., 2017; Ruehr et al., 2019), and an impaired hydraulic system (Brodribb and Cochard, 2009; Brodribb et al., 2010; Skelton et al., 2017) might be the underlying reasons that delayed recovery. The results of our study support

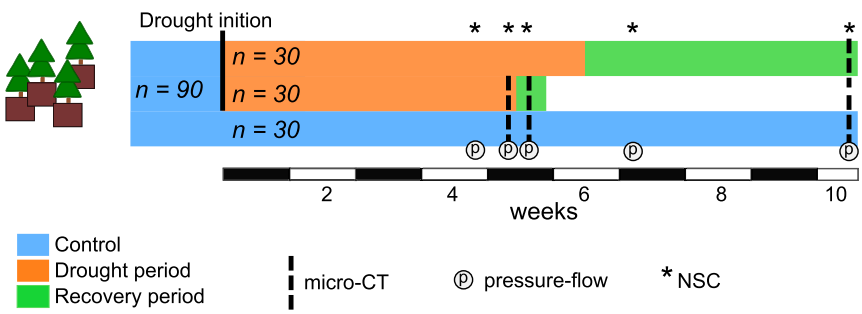

Figure 6. Experimental design. Depicted are the three subsets of seedlings used for (1) a long period of drought recovery (top bar), (2) a short recovery period (middle bar), and (3) control seedlings. The timing of micro-CT, pressure flow, and NSC measurements are indicated.

hydraulic impairment as the most limiting factor of leaf gas exchange recovery, thereby confirming our hypothesis. Following stress release, we found the relationship between Ψ_{Xylem} and leaf gas exchange to differ compared with drought-stress conditions (Fig. 5). In particular, g_s was much lower at the same Ψ_{Xylem} during recovery than before stress was applied. This suggests that leaf gas exchange was primarily limited by the embolism-induced lower hydraulic conductivity post drought. Due to the impaired ability of the seedlings to transport water, stomata could not fully open, which enabled the maintenance of moderate Ψ_{Xylem}. Overall, the 46% reduction of K_S caused by embolism corresponds quite well to transpiration being ~50% lower in drought-recovery compared with control seedlings.

We did not observe K_S recovery within 1 month. This indicates a lack of refilling of embolized tracheids and also points toward a reduced growth of new xylem, albeit NSC concentrations were high. However, since our experiment was conducted during September to November, cambial activity and xylem formation had presumably already stopped at this time of the year (Gruber et al., 2009; Cuny and Rathgeber, 2016). By contrast, one might speculate that a similar experiment earlier during the season could have resulted in K_S recovery (at least partially) along with wood formation. Xylem growth, resulting in the recovery of hydraulic conductance, has been previously observed in conifers (Brodribb et al., 2010; Hammond et al., 2019) and angiosperms (Christensen-Dalsgaard and Tyree, 2014; Skelton et al., 2017). Considering the pine seedlings studied here, we assume that new wood formation in the next growing season would allow for the regain of at least partial hydraulic functioning and an improved overall whole-plant carbon gain, while considering that xylem development typically takes several weeks or even months (Cuny et al., 2014). This is also suggested by a recently developed model that predicts the repair of the hydraulic system to depend on secondary growth of xylem, which is limited by available NSC reserves (Trugman et al., 2018), and tree death would occur if reserves become critically depleted. In a recently developed conceptual framework, the tight coordination between hydraulic and metabolic recovery has been indicated (Ruehr et al., 2019). If stress results in an impaired functionality or tissue damage, recovery will be delayed and depends on repair mechanisms and/or growth of new functional tissue. In our study, we could clearly show that damage to the hydraulic system via embolism formation is not easily repaired and that recovery may rely on the formation of new xylem. This indicates that the intensity of stress and also its frequency can critically affect tree survival, as the production of new functional tissue might be too slow before the onset of the next drought event.

CONCLUSION

Our study demonstrates that a drought causing 50% loss in xylem hydraulic conductivity critically impairs metabolic and hydraulic functioning of Scots pine seedlings. Whereas this did not result in mortality of the seedlings during a 1-month recovery period, it might, in case of lacking recovery, culminate in tree death later on. We found no indication of a recovery of stem hydraulic conductivity and no reversal of xylem embolism either directly after rewetting or 1 month later. These results were supported by both intrusive and nonintrusive methods, and we therefore recommend the application of low-cost intrusive techniques such as pressure-flow measurements and dye-injection experiments to determine hydraulic conductivity and visualize the embolism of conifer xylem. Despite no refilling of embolized tracheids after rewatering, leaf gas exchange partially recovered, which was tightly connected to the reduced water-transport capacity. Moreover, seedlings recovered slowly based on their carbohydrate dynamics, and it needs to be proven if there will be a delayed growth of new xylem.

Our study provides further information on how drought-induced damage of the hydraulic system affects both carbon uptake and NSC dynamics in Scots pine. Based on our findings, we highlight the need for a better physiological understanding of the role of growth processes and carbon reserves in order to predict hydraulic functioning and growth performance after drought. Recent observations (DeSoto et al., 2020) have shown that the mortality of mature trees can be linked to many years of reduced growth performance induced by stress, indicating that an incomplete recovery leaves trees more vulnerable to future drought events.

MATERIALS AND METHODS

Plant Material and Growth Conditions

Potted 2-year-old seedlings of Scots pine (*Pinus sylvestris*; provenance: foothills of the Alps, Germany) were obtained from a local tree nursery and transplanted in larger pots (5 L, 15 cm in diameter, 25 cm in height) in May 2017 in a mixture of fine sand, medium grained sand, gravel, and vermiculite (1:2:1:2). Twelve grams of slow-release fertilizer (Osmocote Exact Standard 5-6M fertilizer 15-9-12+2MgO+TE; ICL Specialty Fertilizers) was added to all pots, supplemented by 0.14 mL of liquid fertilizer [Compo Complete, 6+4+6(+2) NPK(MgO)] to ensure immediate nutrient supply.

Seedlings were grown under controlled conditions in a greenhouse at the Institute of Meteorology and Climate Research in Garmisch-Partenkirchen, Germany (708 miles above sea level, 47°28′32.9′′N, 11°3′44.2′′E). The greenhouse was equipped with highly UV-transmissive glass. To supplement outside light, we used sodium vapor lamps (T-agro 400W; Philips). Air temperature and relative humidity were controlled automatically within the chamber (CC600; RAM Regel- und Messtechnische Apparate), in which ventilation and air-conditioning units allowed for homogenous air conditions. The seedlings were frequently rearranged within the greenhouse compartment. Air temperature and relative humidity were monitored at canopy height with relevant sensors (CS215; Campbell Scientific [enclosed in aspirated radiation shields of type 43502; Young]) alongside the measurement of photosynthetically active radiation (PQS 1; Kipp & Zonen). All seedlings were watered to field capacity every second to third day.

Experimental Design

The drought treatment was initiated on September 1, 2017, by withholding irrigation until a predetermined drought level was reached (Fig. 6). Subsequently,

seedlings were rewatered to field capacity at around 6 PM and watered every second day. During the first 18 d of the drought treatment, day/night oscillation of relative humidity was between 56% ± 8% (mean ± SD) and 72% ± 4%, and air temperature oscillated between 13°C ± 1°C during the night and 20°C ± 5°C during the day (Supplemental Fig. S2). After 18 d, air temperature was increased by approximately 6°C and relative humidity decreased by about 25%, resulting in a maximum vapor pressure deficit of ~3 kPa. During the day, photosynthetically active radiation averaged between 700 and 1,000 μmol m^{-2} s^{-1}. Furthermore, to achieve a predetermined drought level before rewatering, drying was enhanced by ventilators. We targeted a Ψ_{Xylem} causing 40% to 50% PLC to ensure that drought stress would be severe but not lethal, since greater than 50% PLC may lead to mortality in conifers (Brodribb and Cochard, 2009). To estimate this Ψ_{Xylem}, we generated a vulnerability curve using the Cavitron technique (Cochard, 2002; Supplemental Methods S1) and found a P_{50} for Scots pine at −3.01 MPa (P_{12} at −2.42 MPa; Supplemental Fig. S1), which was defined as our target Ψ_{Xylem}.

For micro-CT measurements, a subset of randomly selected control (n = 15) and drought-treated (n = 30) seedlings was transported to the KARA Synchrotron facility near Karlsruhe, Germany (for details, see the "Visualization of Embolism via Micro-CT" section). Measurements were done immediately before and 2 d after rewatering. Between measurements, seedlings were placed outside in natural light conditions, where air temperature ranged between 10°C and 25°C, and relative humidity was 50% to 98% (for details, see Supplemental Fig. S2B). Note that another subset of control (n = 15) and drought-treated (n = 30) seedlings, which had not reached the target Ψ_{Xylem} yet, was left in the greenhouse. These seedlings were rewatered 8 d later when they had reached the target Ψ_{Xylem} (Fig. 6). During the recovery phase, temperature in the greenhouse was about 21°C ± 2°C during the day and 15°C ± 1°C in the night, and relative humidity ranged between 52% ± 6% and 65% ± 6% (Supplemental Fig. S2A), thereby not exceeding a vapor pressure deficit of 1.8 kPa during the day and 1 kPa during the night. To assess if refilling of embolized conduits is a gradual process over time, micro-CT measurements on the second subset of seedlings were conducted 27 d after rewatering. We purposely chose another subset of seedlings to avoid possible artifacts from x-ray radiation on tree health (Cochard et al., 2015; Petruzzellis et al., 2018). Control and drought seedlings scanned via micro-CT were on average 53.3 ± 4.5 and 51.5 ± 3.2 cm in height with stem diameter of ~10.4 ± 1 and 10 ± 0.8 cm, respectively.

Midday Water Potential and RWC_{Needle}

We measured Ψ_{Xylem} from nontranspiring needle fascicles of six control and 10 to 12 drought-recovery seedlings typically at midday directly after leaf gas-exchange measurements (see the "Leaf Gas Exchange" section). Furthermore, Ψ_{Xylem} of all seedlings measured via micro-CT was determined before scanning of seedlings. Transpiration of needles was prevented by enclosing a current-year shoot in a nontransparent plastic bag for 1 h before measurements. Two needle fascicles were sampled from each of the shoots, immediately measured with a Scholander pressure chamber (model 1000 Pressure Chamber Instrument; PMS Instrument), and values were averaged. We tested for agreement between Ψ_{Xylem} from needles of bagged shoots and Ψ_{Xylem} from branches of the same individual and found strong correlation (r = 0.99, $P < 0.001$, n = 6).

During the drought period, Ψ_{Xylem} was measured at time intervals of 2 to 6 d, followed by more frequent measurements when Ψ_{Xylem} reached values closer to the target Ψ_{Xylem}. Directly after rewatering until 2 d later, Ψ_{Xylem} was measured daily. With progression of the recovery period, measurement intervals were prolonged. Assessing Ψ_{Xylem} was often accompanied by measurements of RWC_{Needle}. For this, two needle fascicles per seedling (n = 6 control and n = 10–12 drought-recovery seedlings) were placed in plastic bags to avoid moisture loss, and sample mass was determined immediately (W_{fresh}), after hydrating needles in purified water for 48 h (W_{turgid}), and after drying at 70°C for at least 48 h (W_{dw}). The time until needles were fully hydrated was predetermined by saturation curves for dehydrated and control seedlings. RWC_{Needle} was then calculated according to Chen et al. (2010) as follows:

$$RWC_{Needle}(\%) = 100^{*}\frac{(W_{fresh} - W_{dw})}{W_{turgid} - W_{dw}} \quad (1)$$

Leaf Gas Exchange

Leaf gas-exchange measurement campaigns were coordinated with Ψ_{Xylem} measurements. A_{SAT} (μmol CO_2 m^{-2} s^{-1}), E (mmol m^{-2} s^{-1}), and g_s (mmol m^{-2} s^{-1}) were measured using a portable leaf gas-exchange system (Li-6400; LI-COR) equipped with a light source (6400-40 Leaf Chamber Fluorometer). The same fully developed current-year needle cohorts were measured throughout the experiment, and we only switched to other needle cohorts if signs of damage became obvious. The measured projected needle area was known by filling the leaf cuvette (2 cm^2) completely with needles and avoiding overlap as much as possible. Each measurement campaign lasted from 10 to 12 AM, and leaf gas exchange of six control and 10 to 12 drought-recovery seedlings was measured under predetermined saturated light conditions of 1,200 μmol m^{-2} s^{-1}- photosynthetic photon flux density and a CO^2 concentration of 400 μL L^{-1}. Conditions inside the leaf cuvette were kept constant, with an average leaf temperature of 25.5°C, relative humidity of 46.5%, and vapor pressure deficit of 2 kPa. Five days after rewatering, we resumed leaf gas-exchange measurements of those seedlings that were not measured at the micro-CT facility (Fig. 6, top bar). We calculated WUE_i (in μmol CO_2 mol^{-1} water) as a measure of photosynthetic efficiency as follows:

$$WUE_i = \frac{A_{SAT}}{g_s} \quad (2)$$

NSC Measurements

Plant available carbon reserves were determined by analyzing NSC concentrations in samples of needles, roots, stem bark (including cambium), and stem wood (n = 5–8 per tissue and time step), according to Landhäusser et al. (2018). Collection of samples was coordinated with hydraulic conductivity measurements (see the "Stem Xylem Hydraulic Conductivity" section) and was done in the afternoon (3 to 4 PM) as follows. Samples were immediately microwaved for 120 s to stop enzyme activity (Landhäusser et al., 2018), oven dried at 70°C for 78 h, and then ball milled to fine powder (MM200; Retsch). Approximately 10 mg per sample was extracted in 80% (v/v) ethanol at 90°C for 10 min. The supernatant was used for quantifying NSC by high-performance anion-exchange chromatography with pulsed amperic detection, an ion chromatography method. For starch digestion and quantification, the residual pellet was cleaned and dried at 60°C to eliminate the remaining ethanol. Starch was converted to soluble oligosaccharides by using α-amylase from *Bacillus licheniformis* (Sigma catalog no. A4551) for 2 h at 85°C. Solids were separated by centrifugation at 13,000*g* for 1 min, and glucans in the supernatant were hydrolyzed to Glc with amyloglucosidase from *Aspergillus niger* (Sigma catalog no. ROAMYGLL) for 2 h at 55°C. The resulting product Glc hydrolysate was again quantified by HPLC. Results were multiplied by 0.9 to obtain the starch concentration.

Visualization of Embolism via Micro-CT

To visualize embolized tracheids in secondary xylem of intact plants, we conducted micro-CT measurements at the IMAGING beamline at the KARA Synchrotron of the Karlsruhe Institute of Technology. We performed micro-CT scans of the seedlings (1) after drought stress (n = 12), (2) 2 d after rewatering (recovery; n = 10), and (3) 4 weeks after rewatering using another set of seedlings that had not been exposed to x-ray radiation before (n = 12). Furthermore, (4) we measured control seedlings from both subsets (n = 12) and (5) compared synchrotron-based PLA with the Cavitron vulnerability curve by additionally dehydrating seedlings (n = 15; Supplemental Fig. S1). Note that some of these additionally dehydrated seedlings, which were either stressed until reaching P_{12} values (i.e. Ψ_{Xylem} of −1.5 to −2.4 MPa) or exposed to higher drought stress (Ψ_{Xylem} > –3.6 MPa), were also scanned twice (after drought stress and 2 d after rewatering). This was done in order to determine if the degree of embolism has an influence on potential refilling mechanisms (Supplemental Fig. S4, D, E, K, and L).

Before each micro-CT measurement, we determined Ψ_{Xylem} and leaf gas exchange and then placed each seedling in a custom-built plant holder, which was fixed to an air-bearing stage. Branches and needles were wrapped in cling film to avoid movement that could blur the image. The white-beam spectrum (used for the tomography experiments) was filtered with 1 mm Al. The x-ray projections of the tomography scan were recorded with an indirectly converting x-ray area detector composed of a 200-μm-thick LuAG:Ce scintillator, an Optique Peter white beam microscope providing a magnification of 2×, and a PCO.DIMAX camera with 2,016 × 2,016 pixels, with a physical pixel size of 11 μm. The effective pixel size was 5.5 μm and the effective field of view was 11 × 11.08 mm. For each tomography experiment, 6,000 projections over 360 degrees were taken to increase the available field of view. The distance between the sample and the detector (propagation distance) was set to 230 mm. Scan

time per sample was about 3 min. The tomographies were acquired with a frame rate between 40 and 70 frames per second. During micro-CT scans, we used an infrared camera (PI 450; Optris) to observe stem temperature, which remained approximately between 24°C and 26°C. The scanned region was at a stem height of ~4 to 5 cm above the soil surface, and we marked this area in order to scan seedlings after rewatering at the same height. As soon as all micro-CT scans were completed, seedlings were cut and a sample of the stem (~6 cm) that included the scanned area was dried for about 1 d to produce a fully dehydrated stem cross section (reference scan). Additionally, the piece of the stem above the scanned area was used for further hydraulic measurements (see the "Stem Xylem Hydraulic Conductivity" section). Samples from stem, roots, and needles were taken for NSC analysis (see the "NSC Measurements" section).

Images were reconstructed according to Vogelgesang et al. (2016), and the middle slice per sample was automatically selected for quantitative analysis in ImageJ/Fiji image-processing freeware, a Java-based distribution of ImageJ (www.fiji.sc; Schindelin et al., 2012; Rueden and Eliceiri, 2019). We assessed the percentage of air-filled versus water-filled stem xylem conduits by excluding the pith, the primary xylem, and the resin channels as well as other nonconductive areas as determined by the reference scan. Brightness and contrast were modified for each sample individually to improve the detection of water- versus air-filled conduits and thus estimate PLA. Differentiation into air- versus water-filled tracheids was confirmed by dye staining on the same samples analyzed by micro-CT (Supplemental Methods S2).

Stem Xylem Hydraulic Conductivity

Hydraulic conductivity measurements on stem segments of six to 12 seedlings per treatment were conducted using the pressure-flow method (Sperry and Tyree, 1988). First, stem segments were wrapped in cling film, placed in tightly sealed plastic bags, and kept frozen at −18°C for ~10 d until analyses were conducted. Prior test measurements revealed that freezing of samples had no effect on K_S by correlating K_S from frozen with fresh stem segments of the same individuals ($r = 0.94$, $P < 0.001$, $n = 8$).

For hydraulic conductivity measurements, frozen samples were merged in distilled water and slowly thawed. Finally, they were cut back underwater, the bark was removed at the sample ends, and 2 to 3 mm was cut off at both ends with a sharp carving knife to remove exuded resin, which could interfere with flow measurements. The obtained stem segments were about 6 to 10 cm long and had a diameter of approximately 7 to 9 mm. Up to five samples were fastened to a 5-fold valve (Luer-lock system; neoLab Migge Laborbedarf-Vertriebs), and an infusion bag with distilled, filtered (0.22 μm pore size), and degassed water with a 0.005% (v/v) Micropur water purifier (Katadyn Products) was connected to the water flow system. The measurement pressure was 0.004 MPa, and the flow rate was determined for each stem segment separately using a mass flowmeter (mini-CORI-FLOW M13; Bronkhorst). K_S was calculated based on the cross-sectional area of the xylem and length of the sample. We further tested if K_S differed between controls and samples previously exposed to x-ray radiation. We obtained similar results and thus merged them. To generate a vulnerability curve, we dehydrated additional seedlings ($n = 9$), and PLC was obtained by relating K_S to that of control seedlings (Supplemental Fig. S1).

Data Analyses and Statistics

All data analyses were performed in R version 3.6.1 (R Core Team, 2019). To test for significant differences between the control and drought treatments, we used the Wilcoxon rank-sum test to account for small and unequal sample sizes. Considering several groups, we applied the Kruskal-Wallis test followed by the Bonferroni posthoc analysis. $P < 0.05$ was considered significant. Treatment effects on leaf gas exchange, Ψ_{Xylem}, and RWC_{Needle} were further assessed by fitting linear mixed-effects models (lme; lmerTest package; Kuznetsova et al., 2017) using time and treatment as fixed effects and tree number as a random factor to account for repeated measurements in time. Model selection was based on the Akaike's information criterion corrected for small sample size (AICc), and the model with the lowest AICc (i.e. the most parsimonious model) was selected (Burnham and Anderson, 2002). This was followed by the posthoc Tukey's multiple comparisons test of means (Lenth et al., 2020). Tukey's HSD for significant differences between treatments is reported.

To test for dependencies between Ψ_{Xylem} and gas-exchange parameters (A_{SAT} and g_s), we used regression analyses. We fitted a sigmoidal function to data from prestress and drought. Furthermore, we tested for effects of changes in NSC concentration on hydraulic parameters such as K_S, PLA, Ψ_{Xylem}, and RWC_{Needle} by plotting these variables versus starch and soluble sugar concentrations of the relevant tissues. Furthermore, correlation analyses were performed using Spearman's rank correlation.

For selected variables, the percentage treatment effect (TE) of the drought treatment was calculated as follows:

$$TE(\%) = 100 * \frac{(mean_{drought} - mean_{control})}{mean_{control}} \quad (3)$$

where mean is the treatment average per measurement time point.

Supplemental Data

The following supplemental materials are available.

Supplemental Figure S1. PLC as a function of Ψ_{Xylem} for Scots pine seedlings.

Supplemental Figure S2. Air temperature and relative humidity during the experiment and 3 weeks before initiating drought stress.

Supplemental Figure S3. Tissue-specific relationships of soluble sugars and starch with K_S, PLA, Ψ_{Xylem}, and RWC_{Needle}.

Supplemental Figure S4. Transverse x-ray tomography images of stem xylem of Scots pine seedlings.

Supplemental Figure S5. Transverse sections of micro-CT images and dye-stained stem xylem segments of the same individual.

Supplemental Methods S1. PLC via Cavitron.

Supplemental Methods S2. Dye-staining experiments.

ACKNOWLEDGMENTS

We thank Birgit E. Dämon for assistance with hydraulic measurements and Eliana Häfele and Tamara Wittmann for experimental support and assistance at the synchrotron facility. Furthermore, we are grateful to Daniel Nadal Sala for help with statistical data analyses and to three anonymous reviewers for their constructive feedback on an earlier version of the article.

Received April 6, 2020; accepted August 3, 2020; published August 20, 2020.

LITERATURE CITED

Adams HD, Zeppel MJB, Anderegg WRL, Hartmann H, Landhäusser SM, Tissue DT, Huxman TE, Hudson PJ, Franz TE, Allen CD, et al (2017) A multi-species synthesis of physiological mechanisms in drought-induced tree mortality. Nat Ecol Evol **1:** 1285–1291

Allen CD, Breshears DD, McDowell NG (2015) On underestimation of global vulnerability to tree mortality and forest die-off from hotter drought in the Anthropocene. Ecosphere **6:** art129

Anderegg WRL, Flint A, Huang C, Flint L, Berry JA, Davis FW, Sperry JS, Field CB (2015a) Tree mortality predicted from drought-induced vascular damage. Nat Geosci **8:** 367–371

Anderegg WRL, Schwalm C, Biondi F, Camarero JJ, Koch G, Litvak M, Ogle K, Shaw JD, Shevliakova E, Williams AP, et al (2015b) Pervasive drought legacies in forest ecosystems and their implications for carbon cycle models. Science **349:** 528–532

Birami B, Gattmann M, Heyer AG, Grote R, Arneth A, Ruehr NK (2018) Heat waves alter carbon allocation and increase mortality of Aleppo pine under dry conditions. Front For Glob Change **1:** 8

Bouda M, Windt CW, McElrone AJ, Brodersen CR (2019) In vivo pressure gradient heterogeneity increases flow contribution of small diameter vessels in grapevine. Nat Commun **10:** 5645

Brodersen CR, McElrone AJ, Choat B, Matthews MA, Shackel KA (2010) The dynamics of embolism repair in xylem: In vivo visualizations using high-resolution computed tomography. Plant Physiol **154:** 1088–1095

Brodribb TJ, Bowman DJMS, Nichols S, Delzon S, Burlett R (2010) Xylem function and growth rate interact to determine recovery rates after exposure to extreme water deficit. New Phytol **188:** 533–542

Brodribb TJ, Cochard H (2009) Hydraulic failure defines the recovery and point of death in water-stressed conifers. Plant Physiol **149:** 575–584

Brodribb TJ, McAdam SAM (2013) Abscisic acid mediates a divergence in the drought response of two conifers. Plant Physiol **162:** 1370–1377

Buras A, Schunk C, Zeiträg C, Herrmann C, Kaiser L, Lemme H, Straub C, Taeger S, Gößwein S, Klemmt HJ, et al (2018) Are Scots pine forest edges particularly prone to drought-induced mortality? Environ Res Lett **13:** 025001

Burnham K, Anderson D (2002) Model Selection and Multi-Model Inference. Springer, New York

Canny M (1998) Applications of the compensating pressure theory of water transport. Am J Bot **85:** 897–909

Cano FJ, López R, Warren CR (2014) Implications of the mesophyll conductance to CO_2 for photosynthesis and water-use efficiency during long-term water stress and recovery in two contrasting Eucalyptus species. Plant Cell Environ **37:** 2470–2490

Charra-Vaskou K, Badel E, Burlett R, Cochard H, Delzon S, Mayr S (2012) Hydraulic efficiency and safety of vascular and non-vascular components in *Pinus pinaster* leaves. Tree Physiol **32:** 1161–1170

Charrier G, Delzon S, Domec JC, Zhang L, Delmas CEL, Merlin I, Corso D, King A, Ojeda H, Ollat N, et al (2018) Drought will not leave your glass empty: Low risk of hydraulic failure revealed by long-term drought observations in world's top wine regions. Sci Adv **4:** eaao6969

Charrier G, Torres-Ruiz JM, Badel E, Burlett R, Choat B, Cochard H, Delmas CEL, Domec JC, Jansen S, King A, et al (2016) Evidence for hydraulic vulnerability segmentation and lack of xylem refilling under tension. Plant Physiol **172:** 1657–1668

Chen JW, Zhang Q, Li XS, Cao KF (2010) Gas exchange and hydraulics in seedlings of *Hevea brasiliensis* during water stress and recovery. Tree Physiol **30:** 876–885

Choat B, Badel E, Burlett R, Delzon S, Cochard H, Jansen S (2016) Noninvasive measurement of vulnerability to drought-induced embolism by x-ray microtomography. Plant Physiol **170:** 273–282

Choat B, Brodersen CR, McElrone AJ (2015) Synchrotron x-ray microtomography of xylem embolism in *Sequoia sempervirens* saplings during cycles of drought and recovery. New Phytol **205:** 1095–1105

Choat B, Brodribb TJ, Brodersen CR, Duursma RA, López R, Medlyn BE (2018) Triggers of tree mortality under drought. Nature **558:** 531–539

Choat B, Jansen S, Brodribb TJ, Cochard H, Delzon S, Bhaskar R, Bucci SJ, Feild TS, Gleason SM, Hacke UG, et al (2012) Global convergence in the vulnerability of forests to drought. Nature **491:** 752–755

Choat B, Nolf M, Lopez R, Peters JMR, Carins-Murphy MR, Creek D, Brodribb TJ (2019) Non-invasive imaging shows no evidence of embolism repair after drought in tree species of two genera. Tree Physiol **39:** 113–121

Christensen-Dalsgaard KK, Tyree MT (2014) Frost fatigue and spring recovery of xylem vessels in three diffuse-porous trees in situ. Plant Cell Environ **37:** 1074–1085

Cochard H (2002) A technique for measuring xylem hydraulic conductance under high negative pressures. Plant Cell Environ **25:** 815–819

Cochard H, Delzon S, Badel E (2015) X-ray microtomography (micro-CT): A reference technology for high-resolution quantification of xylem embolism in trees. Plant Cell Environ **38:** 201–206

Cuneo IF, Barrios-Masias F, Knipfer T, Uretsky J, Reyes C, Lenain P, Brodersen CR, Walker MA, McElrone AJ (2020) Differences in grapevine rootstock sensitivity and recovery from drought are linked to fine root cortical lacunae and root tip function. New Phytol nph.16542

Cuny HE, Rathgeber CBK (2016) Xylogenesis: Coniferous trees of temperate forests are listening to the climate tale during the growing season but only remember the last words!. Plant Physiol **171:** 306–317

Cuny HE, Rathgeber CBK, Frank D, Fonti P, Fournier M (2014) Kinetics of tracheid development explain conifer tree-ring structure. New Phytol **203:** 1231–1241

Dalla-Salda G, Fernández ME, Sergent AS, Rozenberg P, Badel E, Martinez-Meier A (2014) Dynamics of cavitation in a Douglas-fir tree-ring: Transition-wood, the lord of the ring? J Plant Hydraul **1:** e005

De Baerdemaeker NJF, Arachchige KNR, Zinkernagel J, Van den Bulcke J, Van Acker J, Schenk HJ, Steppe K (2019) The stability enigma of hydraulic vulnerability curves: Addressing the link between hydraulic conductivity and drought-induced embolism. Tree Physiol **39:** 1646–1664

DeSoto L, Cailleret M, Sterck F, Jansen S, Kramer K, Robert EMR, Aakala T, Amoroso MM, Bigler C, Camarero JJ, et al (2020) Low growth resilience to drought is related to future mortality risk in trees. Nat Commun **11:** 545

Dietze MC, Sala A, Carbone MS, Czimczik CI, Mantooth JA, Richardson AD, Vargas R (2014) Nonstructural carbon in woody plants. Annu Rev Plant Biol **65:** 667–687

Domec JC, Gartner BL (2002) How do water transport and water storage differ in coniferous earlywood and latewood? J Exp Bot **53:** 2369–2379

Domec JC, Lachenbruch B, Meinzer FC (2006) Bordered pit structure and function determine spatial patterns of air-seeding thresholds in xylem of Douglas-fir (*Pseudotsuga menziesii*; Pinaceae) trees. Am J Bot **93:** 1588–1600

Earles MJ, Sperling O, Silva LCR, McElrone AJ, Brodersen CR, North MP, Zwieniecki MA (2016) Bark water uptake promotes localized hydraulic recovery in coastal redwood crown: Localized hydraulic recovery via bark water uptake. Plant Cell Environ **39:** 320–328

Etzold S, Ziemińska K, Rohner B, Bottero A, Bose AK, Ruehr NK, Zingg A, Rigling A (2019) One century of forest monitoring data in Switzerland reveals species- and site-specific trends of climate-induced tree mortality. Front Plant Sci **10:** 307

Galiano L, Timofeeva G, Saurer M, Siegwolf R, Martínez-Vilalta J, Hommel R, Gessler A (2017) The fate of recently fixed carbon after drought release: Towards unravelling C storage regulation in *Tilia platyphyllos* and *Pinus sylvestris*. Plant Cell Environ **40:** 1711–1724

Gleason SM, Wiggans DR, Bliss CA, Young JS, Cooper M, Willi KR, Comas LH (2017) Embolized stems recover overnight in *Zea mays*: The role of soil water, root pressure, and nighttime transpiration. Front Plant Sci **8:** 662

Gruber A, Zimmermann J, Wieser G, Oberhuber W (2009) Effects of climate variables on intra-annual stem radial increment in *Pinus cembra* (L.) along the alpine treeline ecotone. Ann Sci **66:** 503

Hagedorn F, Joseph J, Peter M, Luster J, Pritsch K, Geppert U, Kerner R, Molinier V, Egli S, Schaub M, et al (2016) Recovery of trees from drought depends on belowground sink control. Nat Plants **2:** 16111

Hammond WM, Yu K, Wilson LA, Will RE, Anderegg WRL, Adams HD (2019) Dead or dying? Quantifying the point of no return from hydraulic failure in drought-induced tree mortality. New Phytol **223:** 1834–1843

Hartmann H, Moura CF, Anderegg WRL, Ruehr NK, Salmon Y, Allen CD, Arndt SK, Breshears DD, Davi H, Galbraith D, et al (2018) Research frontiers for improving our understanding of drought-induced tree and forest mortality. New Phytol **218:** 15–28

Hartmann H, Trumbore S (2016) Understanding the roles of nonstructural carbohydrates in forest trees: From what we can measure to what we want to know. New Phytol **211:** 386–403

Holbrook NM, Ahrens ET, Burns MJ, Zwieniecki MA (2001) In vivo observation of cavitation and embolism repair using magnetic resonance imaging. Plant Physiol **126:** 27–31

Johnson DM, McCulloh KA, Woodruff DR, Meinzer FC (2012) Hydraulic safety margins and embolism reversal in stems and leaves: Why are conifers and angiosperms so different? Plant Sci **195:** 48–53

Jonsson M, Bengtsson J, Gamfeldt L, Moen J, Snäll T (2019) Levels of forest ecosystem services depend on specific mixtures of commercial tree species. Nat Plants **5:** 141–147

Kaack L, Altaner CM, Carmesin C, Diaz A, Holler M, Kranz C, Neusser G, Odstrcil M, Jochen Schenk H, Schmidt V, et al (2019) Function and three-dimensional structure of intervessel pit membranes in angiosperms: A review. IAWA J **40:** 673–702

Kagawa A, Sugimoto A, Maximov TC (2006) Seasonal course of translocation, storage and remobilization of ^{13}C pulse-labeled photoassimilate in naturally growing *Larix gmelinii* saplings. New Phytol **171:** 793–803

Klein T, Cohen S, Paudel I, Preisler Y, Rotenberg E, Yakir D (2016) Diurnal dynamics of water transport, storage and hydraulic conductivity in pine trees under seasonal drought. IForest Biogeosciences and Forestry **9:** 710–719

Klein T, Zeppel MJB, Anderegg WRL, Bloemen J, De Kauwe MG, Hudson P, Ruehr NK, Powell TL, von Arx G, Nardini A (2018) Xylem embolism refilling and resilience against drought-induced mortality in woody plants: Processes and trade-offs. Ecol Res **33:** 839–855

Körner C (2019) No need for pipes when the well is dry: A comment on hydraulic failure in trees. Tree Physiol **39:** 695–700

Kuznetsova A, Brockhoff PB, Christensen RHB (2017) lmerTest Package: Tests in linear mixed effects models. J Stat Softw **82:** 10.18637/jss.v082.i13

Lalonde S, Tegeder M, Throne-Holst M, Frommer WB, Patrick JW (2003) Phloem loading and unloading of sugars and amino acids. Plant Cell Environ **26:** 37–56

Landhäusser SM, Chow PS, Dickman LT, Furze ME, Kuhlman I, Schmid S, Wiesenbauer J, Wild B, Gleixner G, Hartmann H, et al (2018) Standardized protocols and procedures can precisely and accurately quantify non-structural carbohydrates. Tree Physiol **38:** 1764–1778

Laur J, Hacke UG (2014) Exploring *Picea glauca* aquaporins in the context of needle water uptake and xylem refilling. New Phytol **203:** 388–400

Leng H, Lu M, Wan X (2013) Variation in embolism occurrence and repair along the stem in drought-stressed and re-watered seedlings of a poplar clone. Physiol Plant **147:** 329–339

Lenth R, Singmann H, Love J, Buerkner P, Herve M (2020) emmeans: Estimated marginal means, aka least-squares means. https://github.com/rvlenth/emmeans

Li S, Feifel M, Karimi Z, Schuldt B, Choat B, Jansen S (2016) Leaf gas exchange performance and the lethal water potential of five European species during drought. Tree Physiol **6:** 179–192

Martínez-Vilalta J, Sala A, Piñol J (2004) The hydraulic architecture of Pinaceae: A review. Plant Ecol **171:** 3–13

Mayr S, Cochard H (2003) A new method for vulnerability analysis of small xylem areas reveals that compression wood of Norway spruce has lower hydraulic safety than opposite wood. Plant Cell Environ **26:** 1365–1371

Mayr S, Schmid P, Beikircher B, Feng F, Badel E (2020) Die hard: Timberline conifers survive annual winter embolism. New Phytol **226:** 13–20

Mayr S, Schmid P, Laur J, Rosner S, Charra-Vaskou K, Dämon B, Hacke UG (2014) Uptake of water via branches helps timberline conifers refill embolized xylem in late winter. Plant Physiol **164:** 1731–1740

McCulloh KA, Johnson DM, Meinzer FC, Lachenbruch B (2011) An annual pattern of native embolism in upper branches of four tall conifer species. Am J Bot **98:** 1007–1015

McDowell NG (2011) Mechanisms linking drought, hydraulics, carbon metabolism, and vegetation mortality. Plant Physiol **155:** 1051–1059

Meinzer FC (2002) Co-ordination of vapour and liquid phase water transport properties in plants. Plant Cell Environ **25:** 265–274

Morris H, Plavcová L, Cvecko P, Fichtler E, Gillingham MAF, Martínez-Cabrera HI, McGlinn DJ, Wheeler E, Zheng J, Ziemińska K, et al (2016) A global analysis of parenchyma tissue fractions in secondary xylem of seed plants. New Phytol **209:** 1553–1565

Muller B, Pantin F, Génard M, Turc O, Freixes S, Piques M, Gibon Y (2011) Water deficits uncouple growth from photosynthesis, increase C content, and modify the relationships between C and growth in sink organs. J Exp Bot **62:** 1715–1729

Nardini A, Salleo S (2000) Limitation of stomatal conductance by hydraulic traits: Sensing or preventing xylem cavitation? Trees (Berl) **15:** 14–24

Nardini A, Savi T, Losso A, Petit G, Pacilè S, Tromba G, Mayr S, Trifilò P, Lo Gullo MA, Salleo S (2017) X-ray microtomography observations of xylem embolism in stems of *Laurus nobilis* are consistent with hydraulic measurements of percentage loss of conductance. New Phytol **213:** 1068–1075

Nobel PS (2020) Physiochemical and Environmental Plant Physiology. Academic Press, London

Petruzzellis F, Pagliarani C, Savi T, Losso A, Cavalletto S, Tromba G, Dullin C, Bär A, Ganthaler A, Miotto A, et al (2018) The pitfalls of *in vivo* imaging techniques: Evidence for cellular damage caused by synchrotron x-ray computed micro-tomography. New Phytol **220:** 104–110

Petty JA, Preston RD (1970) Permeability and structure of the wood of Sitka spruce. Proc R Soc Lond B Biol Sci **175:** 149–166

Pickard WF (2003) The riddle of root pressure. I. Putting Maxwell's demon to rest. Funct Plant Biol **30:** 121–134

Poyatos R, Llorens P, Piñol J, Rubio C (2008) Response of Scots pine (*Pinus sylvestris* L.) and pubescent oak (*Quercus pubescens* Willd.) to soil and atmospheric water deficits under Mediterranean mountain climate. Ann For Sci **65:** 306

R Core Team (2019) R: A Language and Environment for Statistical Computing. R Foundation for Statistical Computing, Vienna

Rehschuh R, Mette T, Menzel A, Buras A (2017) Soil properties affect the drought susceptibility of Norway spruce. Dendrochronologia **45:** 81–89

Reichstein M, Bahn M, Ciais P, Frank D, Mahecha MD, Seneviratne SI, Zscheischler J, Beer C, Buchmann N, Frank DC, et al (2013) Climate extremes and the carbon cycle. Nature **500:** 287–295

Rigling A, Bigler C, Eilmann B, Feldmeyer-Christe E, Gimmi U, Ginzler C, Graf U, Mayer P, Vacchiano G, Weber P, et al (2013) Driving factors of a vegetation shift from Scots pine to pubescent oak in dry alpine forests. Glob Change Biol **19:** 229–240

Rueden CT, Eliceiri KW (2019) ImageJ for the next generation of scientific image data. Microsc Microanal **25:** 142–143

Ruehr NK, Grote R, Mayr S, Arneth A (2019) Beyond the extreme: Recovery of carbon and water relations in woody plants following heat and drought stress. Tree Physiol **39:** 1285–1299

Salleo S, Trifilò P, Esposito S, Nardini A, Lo Gullo MA (2009) Starch-to-sugar conversion in wood parenchyma of field-growing *Laurus nobilis* plants: A component of the signal pathway for embolism repair? Funct Plant Biol **36:** 815–825

Salmon Y, Torres-Ruiz JM, Poyatos R, Martinez-Vilalta J, Meir P, Cochard H, Mencuccini M (2015) Balancing the risks of hydraulic failure and carbon starvation: A twig scale analysis in declining Scots pine. Plant Cell Environ **38:** 2575–2588

Schindelin J, Arganda-Carreras I, Frise E, Kaynig V, Longair M, Pietzsch T, Preibisch S, Rueden C, Saalfeld S, Schmid B, et al (2012) Fiji: An open-source platform for biological-image analysis. Nat Methods **9:** 676–682

Schwalm CR, Anderegg WRL, Michalak AM, Fisher JB, Biondi F, Koch G, Litvak M, Ogle K, Shaw JD, Wolf A, et al (2017) Global patterns of drought recovery. Nature **548:** 202–205

Skelton RP, Brodribb TJ, McAdam SAM, Mitchell PJ (2017) Gas exchange recovery following natural drought is rapid unless limited by loss of leaf hydraulic conductance: Evidence from an evergreen woodland. New Phytol **215:** 1399–1412

Skelton RP, West AG, Dawson TE (2015) Predicting plant vulnerability to drought in biodiverse regions using functional traits. Proc Natl Acad Sci USA **112:** 5744–5749

Sperry JS, Tyree MT (1988) Mechanism of water stress-induced xylem embolism. Plant Physiol **88:** 581–587

Taiz L, Zeiger E, Møller IM, Murphy AS (2014) Plant Physiology and Development. Sinauer Associates, Sunderland, MA

Tomasella M, Häberle KH, Nardini A, Hesse B, Machlet A, Matyssek R (2017) Post-drought hydraulic recovery is accompanied by non-structural carbohydrate depletion in the stem wood of Norway spruce saplings. Sci Rep **7:** 14308

Tomasella M, Petrussa E, Petruzzellis F, Nardini A, Casolo V (2019) The possible role of non-structural carbohydrates in the regulation of tree hydraulics. Int J Mol Sci **21:** 144

Torres-Ruiz JM, Cochard H, Mencuccini M, Delzon S, Badel E (2016) Direct observation and modelling of embolism spread between xylem conduits: A case study in Scots pine. Plant Cell Environ **39:** 2774–2785

Trugman AT, Detto M, Bartlett MK, Medvigy D, Anderegg WRL, Schwalm C, Schaffer B, Pacala SW (2018) Tree carbon allocation explains forest drought-kill and recovery patterns. Ecol Lett **21:** 1552–1560

Tyree MT, Sperry JS (1989) Vulnerability of xylem to cavitation and embolism. Annu Rev Plant Biol **40:** 19–36

Umebayashi T, Morita T, Utsumi Y, Kusumoto D, Yasuda Y, Haishi T, Fukuda K (2016) Spatial distribution of xylem embolisms in the stems of *Pinus thunbergii* at the threshold of fatal drought stress. Tree Physiol **36:** 1210–1218

Usta I, Hale MD (2006) Comparison of the bordered pits of two species of spruce (Pinaceae) in a green and kiln-dried condition and their effects on fluid flow in the stem wood in relation to wood preservation. Forestry **79:** 467–475

Utsumi Y, Sano Y, Funada R, Ohtani J, Fujikawa S (2003) Seasonal and perennial changes in the distribution of water in the sapwood of conifers in a sub-frigid zone. Plant Physiol **131:** 1826–1833

Vandegehuchte MW, Bloemen J, Vergeynst LL, Steppe K (2015) Woody tissue photosynthesis in trees: Salve on the wounds of drought? New Phytol **208:** 998–1002

Vogelgesang M, Farago T, Morgeneyer TF, Helfen L, Dos Santos Rolo T, Myagotin A, Baumbach T (2016) Real-time image-content-based beamline control for smart 4D x-ray imaging. J Synchrotron Radiat **23:** 1254–1263

Watson JEM, Evans T, Venter O, Williams B, Tulloch A, Stewart C, Thompson I, Ray JC, Murray K, Salazar A, et al (2018) The exceptional value of intact forest ecosystems. Nat Ecol Evol **2:** 599–610

Weber R, Gessler A, Hoch G (2019) High carbon storage in carbon-limited trees. New Phytol **222:** 171–182

Wheeler JK, Huggett BA, Tofte AN, Rockwell FE, Holbrook NM (2013) Cutting xylem under tension or supersaturated with gas can generate PLC and the appearance of rapid recovery from embolism. Plant Cell Environ **36:** 1938–1949